

# Coupled-bunch instability in the Fermilab Main Injector: Longitudinal-phase-space simulation

F. Rivera-Medero

*Fermi National Accelerator Laboratory\**

*P.O. Box 500, Batavia, IL 60510*

## Abstract

The Fermilab Main Injector is a multi-purpose 150 GeV proton synchrotron. It is designed to provide beams up to  $3 \times 10^{13}$  protons (in up to 504 bunches) at 120GeV to the Switchyard experimental areas,  $3 \times 10^{13}$  protons at 150GeV for the Tevatron fixed target experiments and high intensity ( $3.5 \times 10^{11}$  protons/bunch) in 36 bunches or more for Tevatron collider operation. The accelerator consists of 18 recycled Main Ring rf cavities which operate at a harmonic number 588. These cavities are known to have many high Q resonances. Longitudinal coupled bunch instability in the beam induced by excitation of these higher order resonances may become a serious problem to increase the beam intensity in the MI. Here we present the results of our preliminary study of longitudinal coupled bunch instability in the Main Injector with 84 and 504 bunches using simulation code ESME. The simulations have been carried out by including space charge effects, beam pipe broad impedance and four observed high Q resonances of the MI rf cavities below 350 MHz.

---

\*Operated by the Universities Research Association, under contract with the U.S. Department of Energy

## I. INTRODUCTION

### A. Overview

The Fermilab Main Injector (FMI) [1] is a high energy, high intensity proton synchrotron. A synchrotron is a particle accelerator or storage ring where particles follow a closed loop established by dipole magnetic field, and particles are held together by focusing quadrupole magnets arranged in FODO lattice. Sextupoles and other multipoles provide chromaticity and other higher order corrections to the beam.

In the FMI, the protons and antiprotons are accelerated in bunches by electric fields in radio frequency (rf) cavities operating at about 53 MHz. There are 18 rf cavities in the MI which are recycled from the Main Ring (old accelerator). The maximum number of bunches possible in the FMI at a particular time is 588 (harmonic number of the MI). In the main Injector, a beam up to  $3 \times 10^{13}$  protons/batch can be accelerated from 8.889 GeV/c to 150 GeV/c in less than two seconds.

Recent studies carried out at Fermilab Main Ring [2,3] indicated that the beam intensity was severely limited by the longitudinal coupled bunch instability arising from the excitation of the higher order resonances of MR rf cavities by the wake field left by the leading bunches of the beam. Since MI uses the same rf cavities, it is highly essential to investigate the longitudinal coupled bunch instability in the Main Injector for a different operating scenario.

### B. Longitudinal beam dynamics [4-6]

Half a century ago, V. Veksler and E. McMillan demonstrated how ensembles of charged particles (*bunches*) with a small momentum spread around some *synchronous momentum*  $P_s$  may be accelerated at nearly constant orbit radius, in an increasing magnetic guide field. The accelerating fields are generated by radio frequency resonant cavities operating at a frequency  $\omega_{rf}/(2\pi)$  equal to an integer  $h$  (*harmonic number*) times the revolution frequency

$\omega_s/(2\pi)$  of the synchronous particle i.e.,

$$\omega = h\omega_s = \frac{h\beta_s c}{R}$$

where  $R$  is the average radius of the accelerator and  $\beta_s c$  is the velocity of the synchronous particle. Throughout this work the synchronous trajectory is assumed to lie on the central orbit so that  $R \equiv r_s$ . The voltage across the gap of the accelerating cavity is given by

$$V(t) = \hat{V} \sin\phi(t)$$

where  $\phi$  is the phase angle. The average bending field  $B_s$  on the synchronous particle is given by

$$B_s = \frac{P_s}{eR}.$$

The energy gain of the synchronous particle in one turn is

$$\Delta E_s = e\hat{V} \sin\phi_s = 2\pi e R^2 \dot{B}_s.$$

These are the equations for a synchronous particle. Non-synchronous particles in the bunch have energy, orbit radius, etc., that differ from the synchronous values by the small amounts

$$\begin{aligned} r &= r_s + \Delta r, & \phi &= \phi_s + \Delta\phi, \\ P &= P_s + \Delta P, & E &= E_s + \Delta E, \\ \theta &= \theta_s + \Delta\theta, \end{aligned}$$

where  $\theta$  is the azimuthal angle around the machine. We have

$$\Delta\phi = -h\Delta\theta, \quad \Delta\omega = -\frac{1}{h} \frac{d\phi}{dt}.$$

The slip factor  $\eta$  is an important quantity in longitudinal motion. It is given by

$$\eta \equiv -\frac{d\omega/\omega}{dP/P} = \frac{1}{\gamma_t^2} - \frac{1}{\gamma^2}$$

where  $\gamma_t$  is the transition energy of the synchrotron. Transition energy is reached when  $\eta = 0$ . Qualitatively,  $\gamma_t$  is the energy at which an accelerated particle becomes a relativistic

particle, although this change is gradual, it is most noticeable when the energy approaches  $\gamma_t$ .

The equations of motion for non-synchronous particles are

$$\begin{aligned}\frac{d}{dt}\left(\frac{\Delta E}{\omega_s}\right) &= \frac{e\hat{V}}{2\pi}[\sin\phi - \sin\phi_s] \\ \frac{d\phi}{dt} &= \frac{h\eta\omega_s}{P_s R}\left(\frac{\Delta E}{\omega_s}\right).\end{aligned}$$

Combining these two equations and neglecting the change in momentum and work with small phase deviations we get the simplified linearized equation of small amplitude synchrotron oscillations

$$\frac{d^2}{dt^2}(\Delta\phi) - \frac{e\hat{V}\eta\omega_s\cos\phi_s}{2\pi P_s R} = 0.$$

## Phase Stability

The basic mechanism of phase stability has much in common with simple harmonic motion. Below transition, a lagging particle gains energy with respect to the synchronous particle at the crossing of the rf cavity. This causes it to speed up and overtake the synchronous particle. This energy gain will make the particle arrive at the gap earlier than the synchronous particle and thus it will receive less energy from the cavity. The process reverses after transition. That is, the particle which gets the larger energy kick arrives at the gap at a later phase on the next turn.

To maintain phase stability during acceleration across transition energy, the synchronous phase must switch from  $0 < \phi_s < \frac{1}{2}\pi$  to  $\frac{1}{2}\pi < \phi_s < \pi$ . When  $V_{rf} > 2\pi\frac{dp_s}{dt}\beta_s c/e\omega_s$  and  $0 < \sin\phi_s < 1$  then there is a range of  $\phi$  and  $\delta$  for which the particles have stable synchrotron oscillations. The stable region which determines the maximum possible extent of a bunch is referred to as an rf bucket. The phase-space area occupied by a bunch of particles is referred to as *longitudinal emittance*.

The tune of the synchrotron oscillations, denoted by  $\nu$  is defined

$$\nu \equiv \frac{\Omega_{syn}}{\omega_s},$$

where  $\Omega_{syn}$  is the small amplitude synchrotron oscillation frequency

$$\Omega_{syn} = \sqrt{\frac{e\hat{V}|\eta|\omega_s \cos\phi_s}{2\pi P_s R}}.$$

Near transition, as  $\eta$  approaches zero, so does  $\Omega_{syn}$  and synchrotron oscillations freeze.

### C. Coupled bunch instabilities [7,8]

During acceleration of bunches of particles, several instabilities may arise due to the interaction of the beam with its environment. As a proton bunch passes through an rf cavity, it excites several resonant modes, leaving energy in the cavity. If this excitation, or as it may be called, wakefield, persists until the arrival of subsequent bunches, longitudinal coupled bunch instability may be induced. Coupled bunch motion might continue to grow exponentially until a mechanism such as Landau damping limits further growth. Collective coupled bunch instabilities are counteracted by Landau damping from synchrotron frequency spread  $\Delta\nu$  within the bunch. This damping is obtained if the mode frequency lies within the effective spread of the bunch.

Although the resonances may in general couple both longitudinal and transverse motion, we consider here only the longitudinal coupling impedance

$$Z_{||}(\omega) = -\frac{V_{||}(\omega)}{I_B(\omega)}$$

where  $V_{||}(\omega)$  is the longitudinal voltage per turn induced in the beam and  $I_B(\omega)$  is the fourier amplitude of the beam current at a frequency  $\omega$ .

The impedance due to the rf cavities may consist of sharp peaks at resonant frequencies corresponding to the cavity modes. Besides being driven at their fundamental accelerating mode, the cavities will be driven at higher order parasitic modes.

The longitudinal component of the impedance caused by any mode is

$$Z_{||}(\omega) = \frac{R_S}{[1 + iQ(\frac{\omega_R}{\omega} - \frac{\omega}{\omega_R})]}$$

In this equation  $\omega_R = 2\pi f_R$  is the resonance angular frequency and  $R_S$  is the strength, or shunt impedance, of the longitudinal mode expressed in ohms.

For  $M$  equally spaced coupled bunches there are  $M$  possible dipole modes labeled by  $m = 1, 2, \dots, M$  [8]. With the azimuthal position of the centroid of each bunch,  $\theta_l$ ,  $l = 1, 2, \dots, M$ . The signature of the simplest coupled bunch mode is given by

$$\theta_l(t) = \theta_0 \sin(2\pi ml/M - \omega_s t)$$

and has the form of a discrete propagating plane wave. In addition, an individual bunch in the  $m$ -th coupled bunch mode requires an index “ $n$ ” to describe its motion in synchrotron phase space, e. g. the dipole mode,  $n = 1$ , where the bunches move rigidly as they execute longitudinal synchrotron oscillations.

A simple resonant condition for the  $m$ th dipole mode driven by the longitudinal impedance  $Z(\omega)$  sharply peaked at  $\omega_c$  would be

$$\omega_c = (nM + m)\omega_{\pm}\omega_s$$

where  $n$  is an integer. From this we can see that the resonance condition exists on a limited time interval.

In the past, many higher order resonances have been observed in the MR (now in MI) rf cavities [9]. The measured modes of the cavity without cavity bias and with cavity bias are shown in Fig. 1. Passive and active dampers have been developed to reduce (so called “dQ-ing”) the effect of some of the important modes viz., one at 127 MHz and another at 227 MHz.

Recently, during 1996-98 Fermilab fixed target experiment, one of us (CMB) has observed that with 1008 bunches in the Main Ring, at bunch intensity of the order of  $2.48 \times 10^{10}$  protons, the resonance at about 82 MHz starts contributing to the total beam impedance. This

resonance might introduce instability in the beam. In the present investigation, we select four prominent modes below 350 MHz and tried to study the effect of all of them in accelerating 84-504 bunches in the Main Injector. The measured Q-values and shunt impedances with the above mentioned dampers are listed in Table 1. The study of coupled bunch instability is carried out using multi-particle longitudinal beam dynamics simulation computer code ESME [10-13].

MI rf impedance data used in ESME simulations

frequency(MHz)	Impedance( $\Omega$ )	Q
$f_R$	$R_S$	
82.253	20980.0	2734
127.25	7140.0	241
197.776	944.4	100
227.549	20790.0	456
261.996	1041.0	100
336.876	987.0	687
(Broad Band - beam pipe Impedance)		
2.177E03	0.72282E5	1

Table 1: Shunt Impedance in the FMI cavities

#### D. Longitudinal phase-space tracking code (ESME)

The longitudinal particle tracking code ESME is used to study time evolution in phase space of a beam undergoing instabilities. ESME was developed [10-13] in Fermilab. The tracking procedure used is a turn by turn iteration of two Hamilton-type difference equations describing synchrotron oscillation in  $\theta - \epsilon$  phase space. In order to include the effect of the beam environment one can consider the additional potential due to the wakefield generated

by the beam as it passes through the vacuum pipe. Knowing the particle distribution in the azimuthal direction  $\rho(\theta)$  and the revolution frequency  $\omega_0$  after each turn, one can construct a wakefield induced voltage as follows:

$$V_i(\omega) = e\omega_0 \sum_n \rho_n Z(n\omega_0) e^{in\theta}$$

where  $\rho_n$  represents the discrete Fourier spectrum of the beam and  $Z(\omega)$  is longitudinal coupling impedance. The equations used by ESME are:

$$\theta_{i,n} = \left[ \frac{\tau_{s,n-1}}{\tau_{s,n}} \theta_{i,n-1} + 2\pi \left( \frac{\tau_{i,n}}{\tau_{s,n}} - 1 \right) \right]_{\text{mod}(\pi)}$$

$$E_{i,n} = E_{i,n-1} + eV(\phi_{s,n} + h\theta_{i,n}) - eV(\phi_{s,n})$$

The results may be viewed in time domain or in frequency domain, passing from one to the other through Fast Fourier Transforms.

## II. ESME SIMULATIONS AND RESULTS

In order to simulate the effects of the environment on the beam we assume that the MI is a circular accelerator (originally oval shaped) with an average radius  $R = 528.302$  meters. The space charge effect is included in the simulation, which has the form

$$\left( \frac{Z_{||}}{n} \right)_{\text{space-charge}} = i \frac{377}{2\beta\gamma^2} \left[ 1 + 2\ln \frac{b}{a} \right] [\text{Ohm}]$$

where  $b$  is the average beam pipe radius and  $a$  is the average beam size,  $\beta$  and  $\gamma$  are the relativistic quantities  $v/c$  and  $E/cm_o c^2$ . In the present calculations, the MI beam pipe is assumed to have an average radius of 0.058 meters. The beam is assumed to have a radius of 0.005 meters. Other relevant parameters are listed in Table 2.

The impedance data measured from one rf cavity are collected from ref.[6] (see Table 1). In the calculation we assume the total cavity impedance is 18 times the single cavity impedance. The broad band impedance of the MI is assumed to be  $3\Omega$ , which is about a factor of two higher than the original projection [13].



ESME calculations have been carried out on two configurations of bunches, viz, one Booster batch of 84 bunches and 6 Booster batches to a total of 504 bunches in the accelerator. In both cases we take 200 macro-particles per bunch, where each particle is assumed to have an electronic charge of  $3 \times 10^8 e$ , for simulation. The tracking is carried out from injection momentum of 8.889 GeV/c to 120 GeV/c. The first case is important for the  $\bar{p}$  production cycle, and the second scenario is relevant to the fixed target operation mode of the MI.

Table 2. The Main Injector parameters.

Description	Values
Mean radius of FMI	528.3019 m
$\gamma_t$ (nominal)	21.838
$\dot{\gamma}_t$	267 sec <sup>-1</sup>
$\alpha_1^a$	0.002091
Maximum RF Frequency	53 MHz
Maximum RF Voltage	4 MV
Longitudinal Emittance	0.15 eV-sec
Bunch Intensity	$6 \times 10^{10}$
Number of Bunches	84 to 504
Broad Band coupling impedance $Z_{  }/n$	3 $\Omega$
Beam pipe wave guide cutoff frequency	1.5–2.2 GHz cutoff
Transverse Beam size(a)	0.005 m
Beam pipe Radius (b)	0.058 m

To populate the bunches in the Main Injector we have used a special routine in ESME called SHAZAM 6 routine. This is a facility intended to allow users to integrate their own routines into the code. It was modified to include the effects of coupled bunch modes for up to 588 bunches since the original program would only allow up to 84 bunches.

The simulation results are presented in Figs. 2 to 7 for the cases of 504 bunches. The results of calculations for 84 bunches are displayed in Figs. 8 to 13. In the first set of figures we compare the first three and last three bunches and, their mountain range pictures, at different times in the acceleration cycle. Mountain range pictures are plots that resemble mountains. They illustrate time evolution of a distribution as a function of  $\theta$ . They consist of traces taken every 40 turns for the 504 bunch situation and every 324 turns for the 84 bunch scenario. Transition was taken to be at 0.2 seconds. As is clearly seen the head is minimally affected. Whereas the tail is maximally affected, and there is significant emittance growth. We do not see beam losses under any case. The cases for 84 bunches we find that the emittance growth is of the order of 30%.

# FIGURES

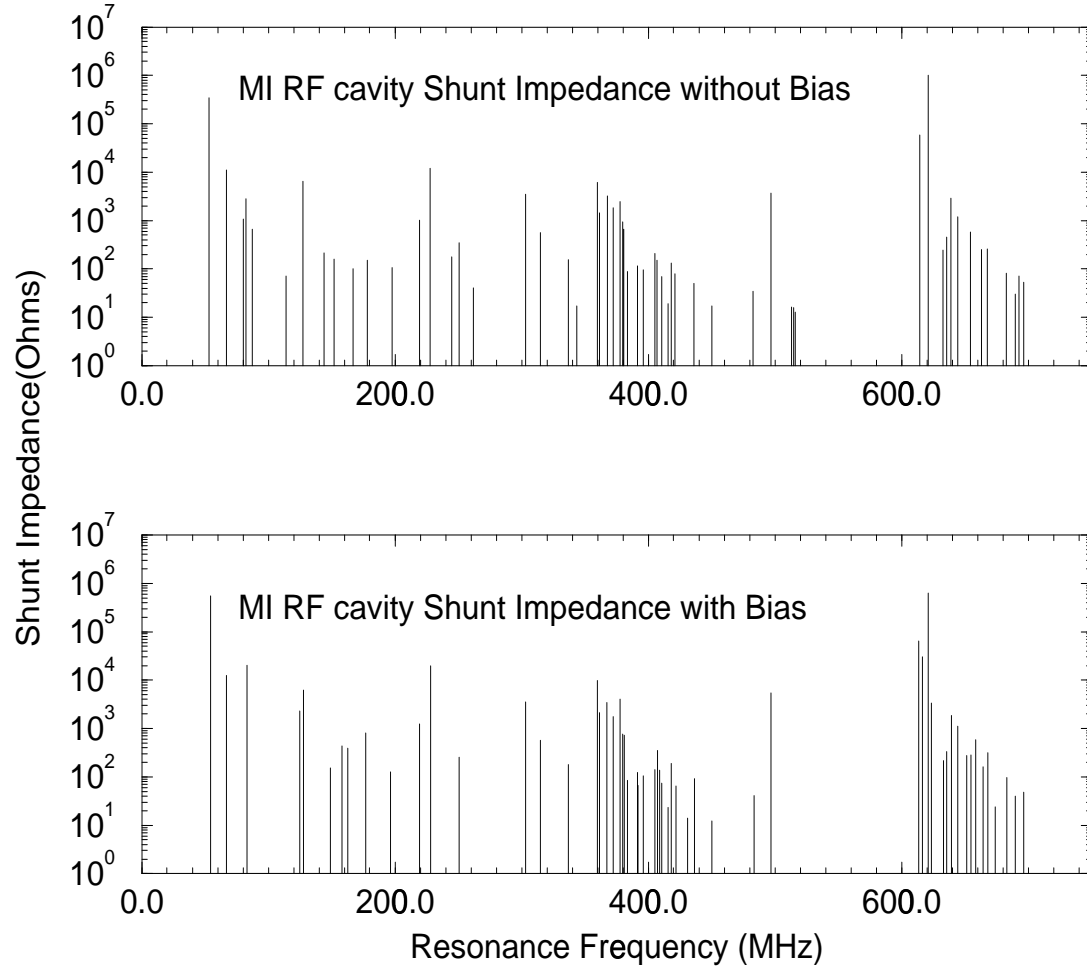


FIG. 1. Shunt Impedance vs. Frequency[6]

ESME Output

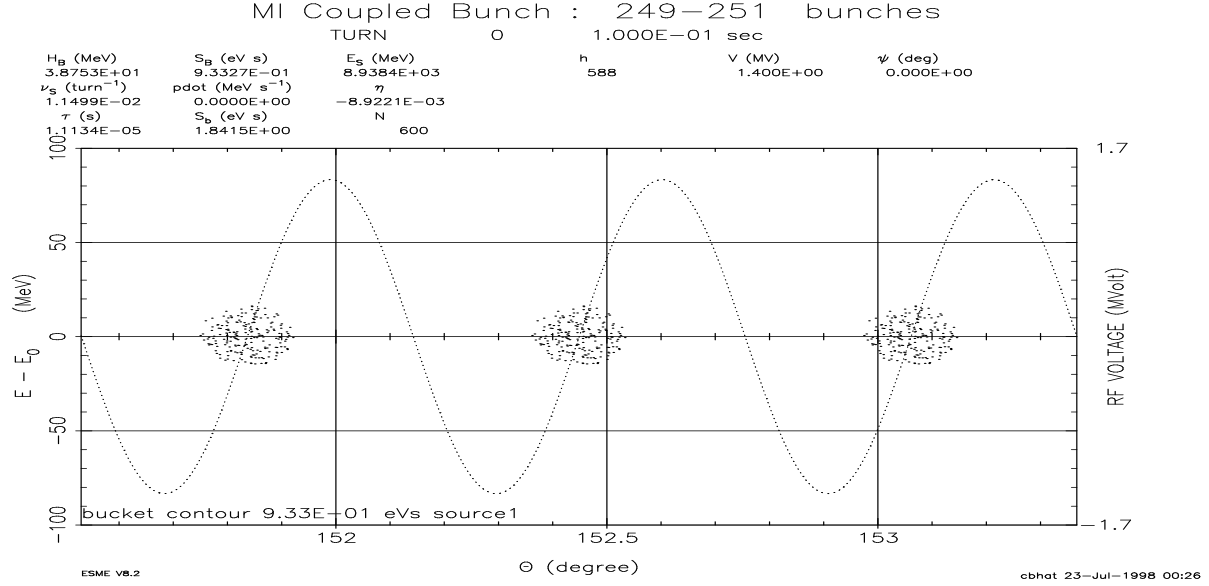
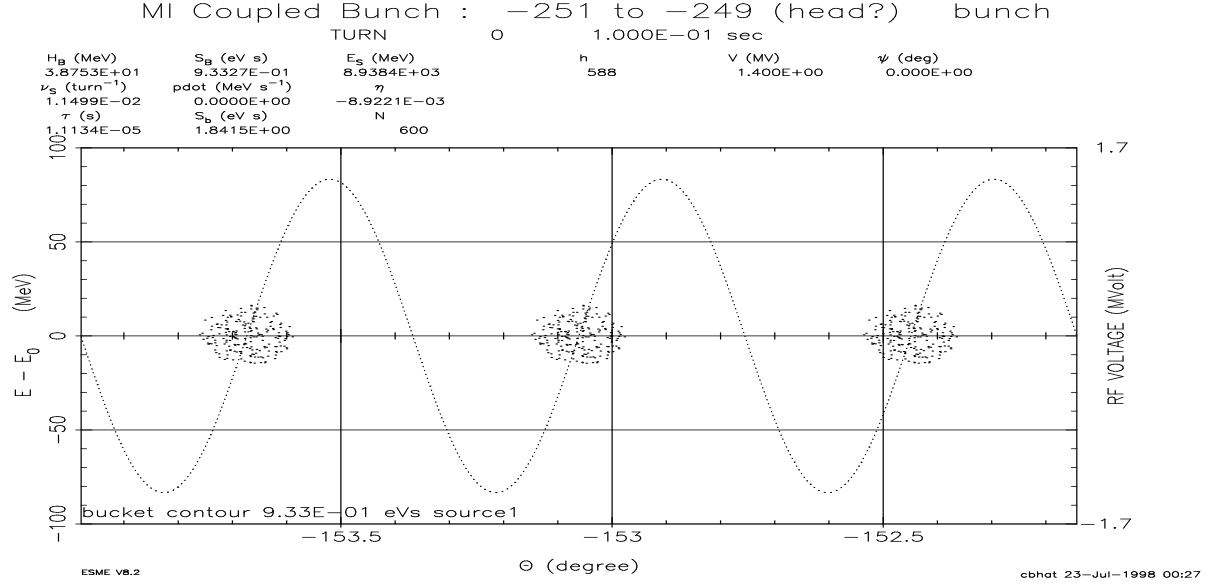


FIG. 2. Phase space distribution of (top) first three and (bottom) last three bunches in a train of 504 bunches in the Main Injector at injection with an energy of 8.9384GeV

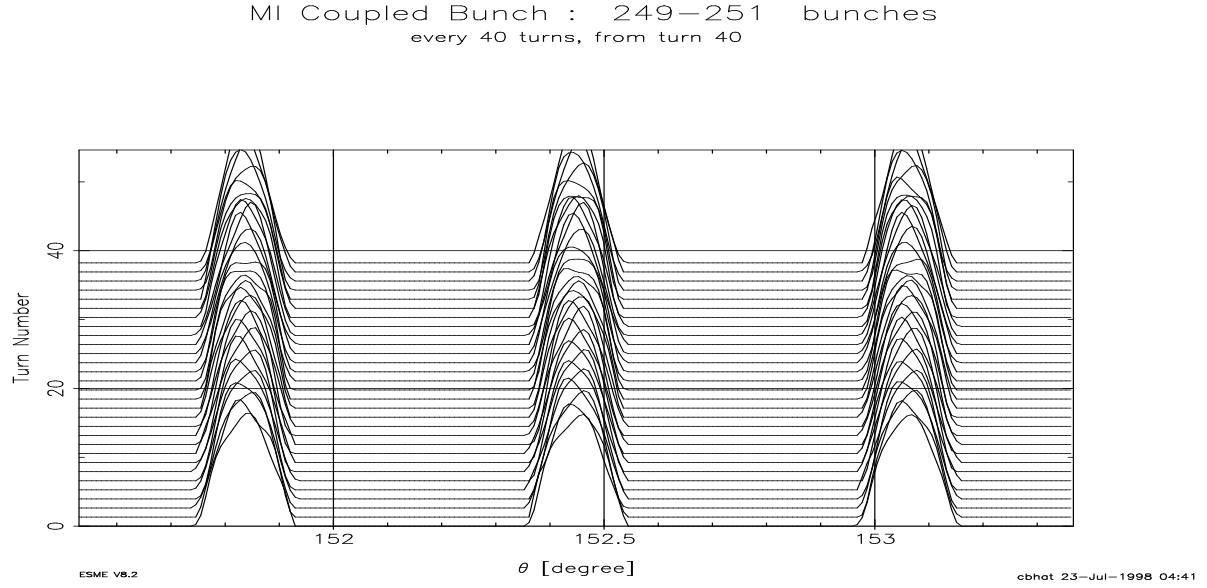
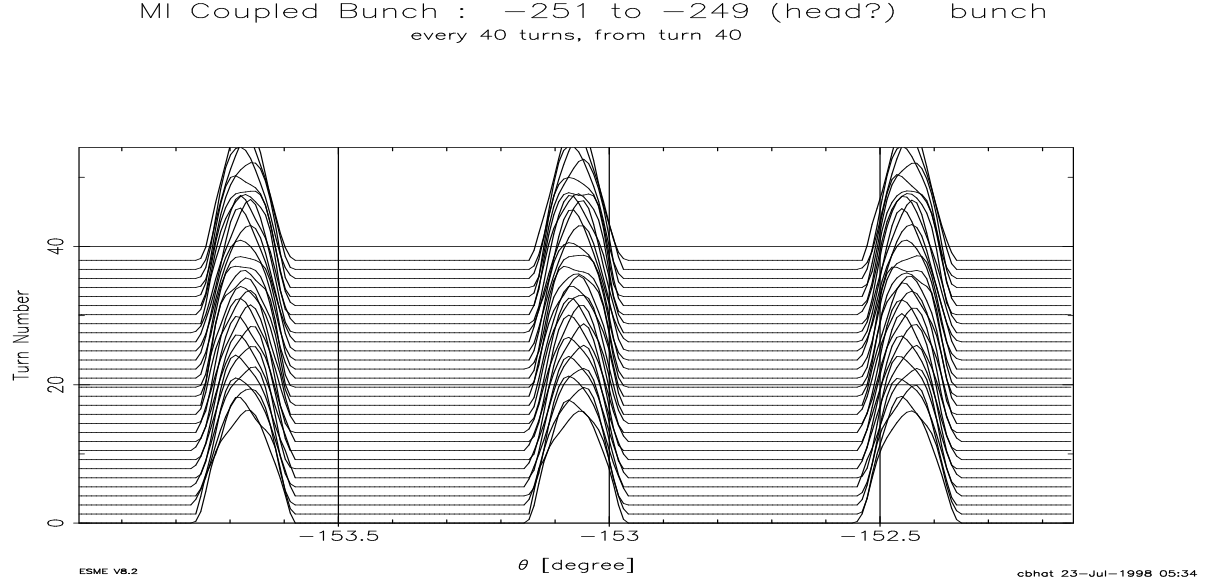


FIG. 3. Mountain range plots illustrating change in bunch length of (top) first three and (bottom) last three bunches in a train of 504 bunches in the Main Injector at injection (40 revolutions per trace).

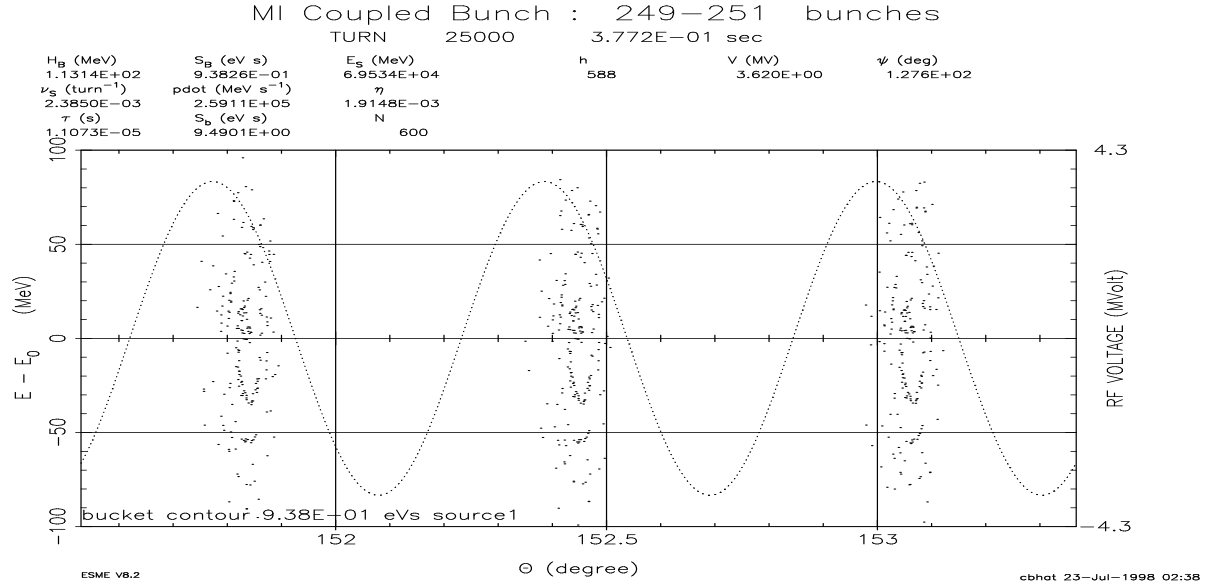
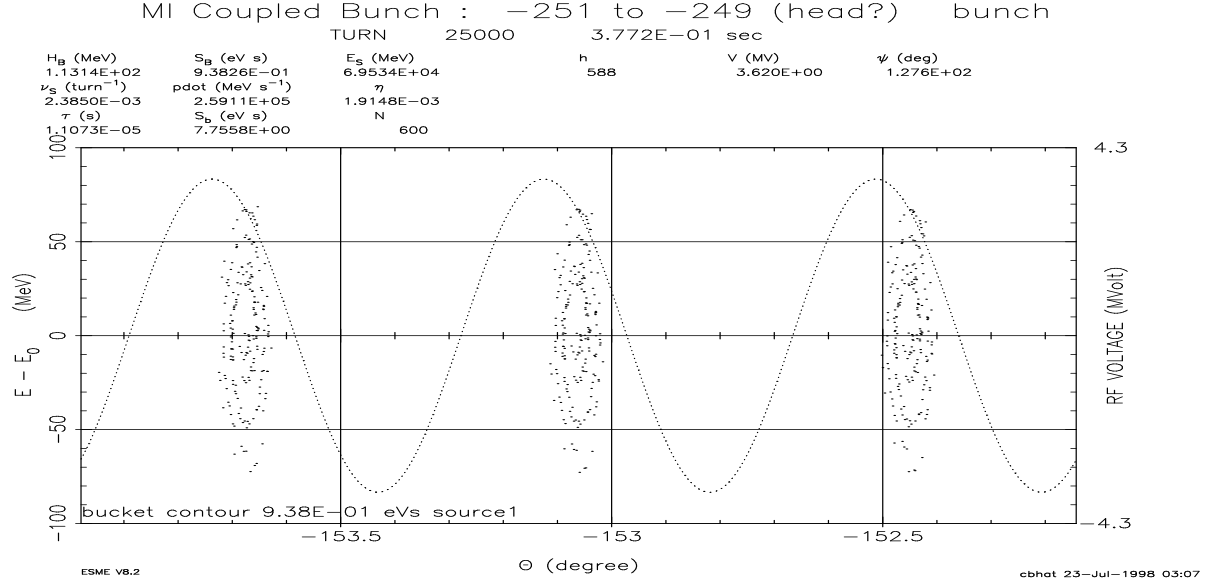


FIG. 4. Phase space distribution (top) first three and (bottom) last three bunches in a train of 504 bunches in the Main Injector after 0.365 seconds of acceleration.

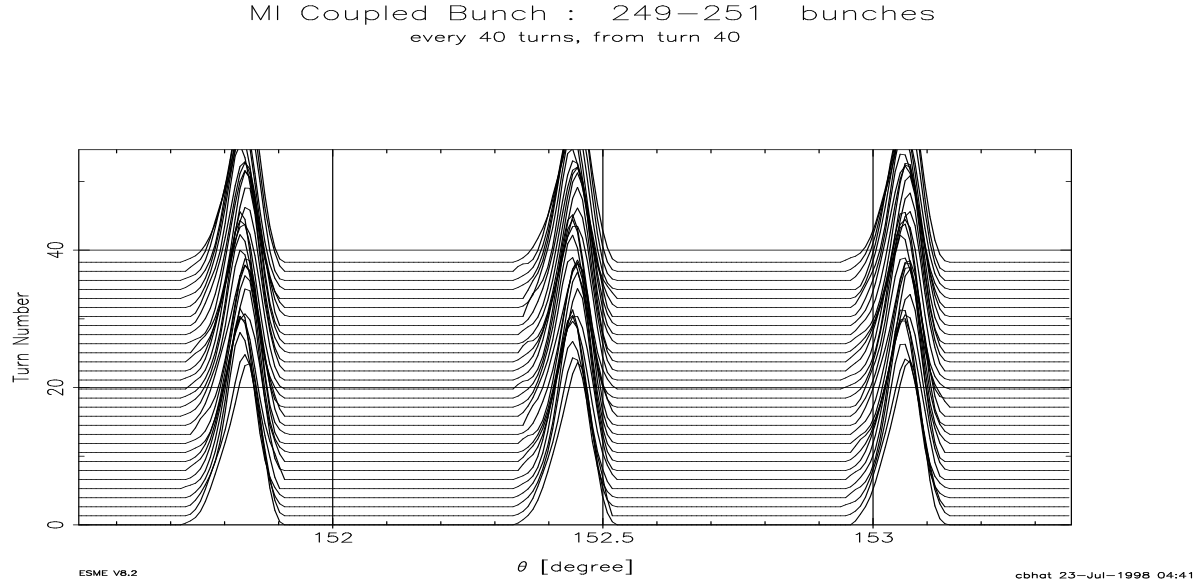
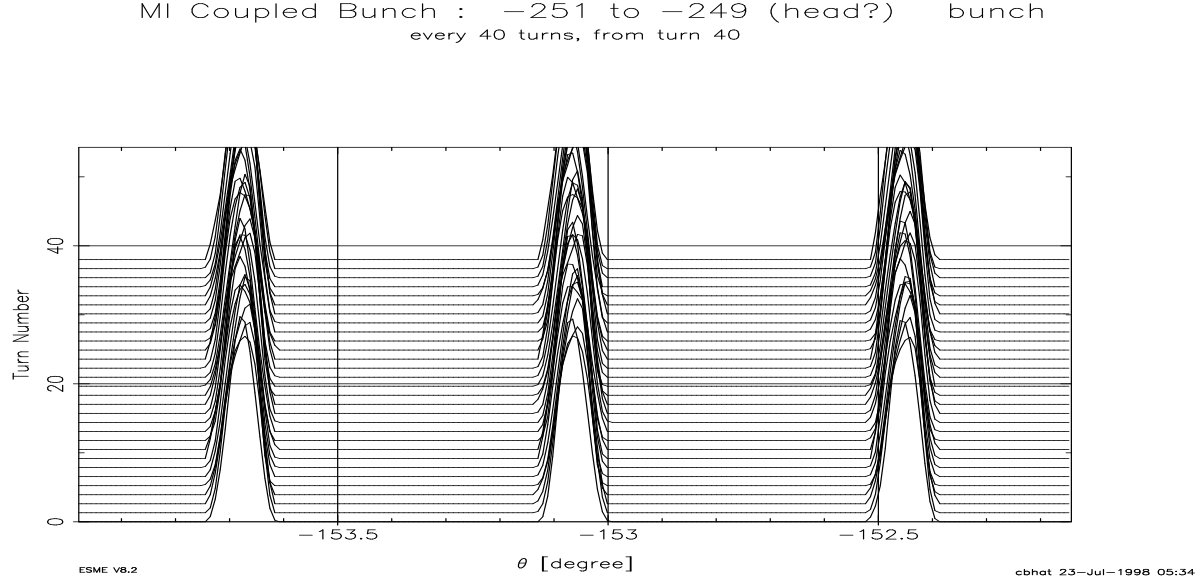


FIG. 5. Mountain range plots illustrating change in bunch length of (top) first three and (bottom) last three bunches in a train of 504 bunches in the Main Injector after 0.365 seconds (40 revolutions per trace).

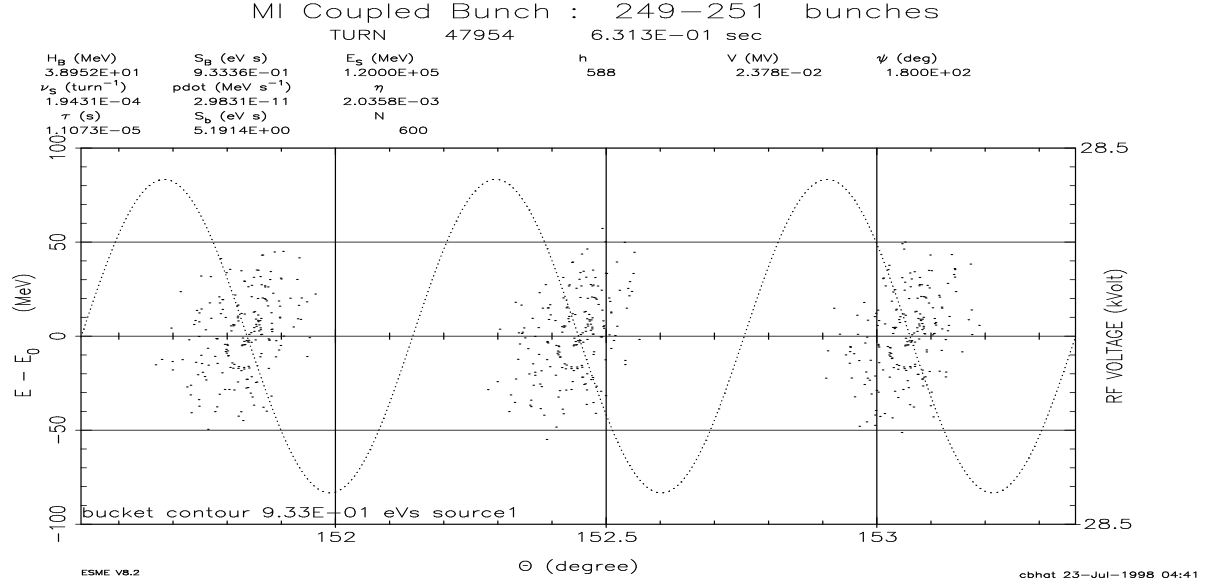
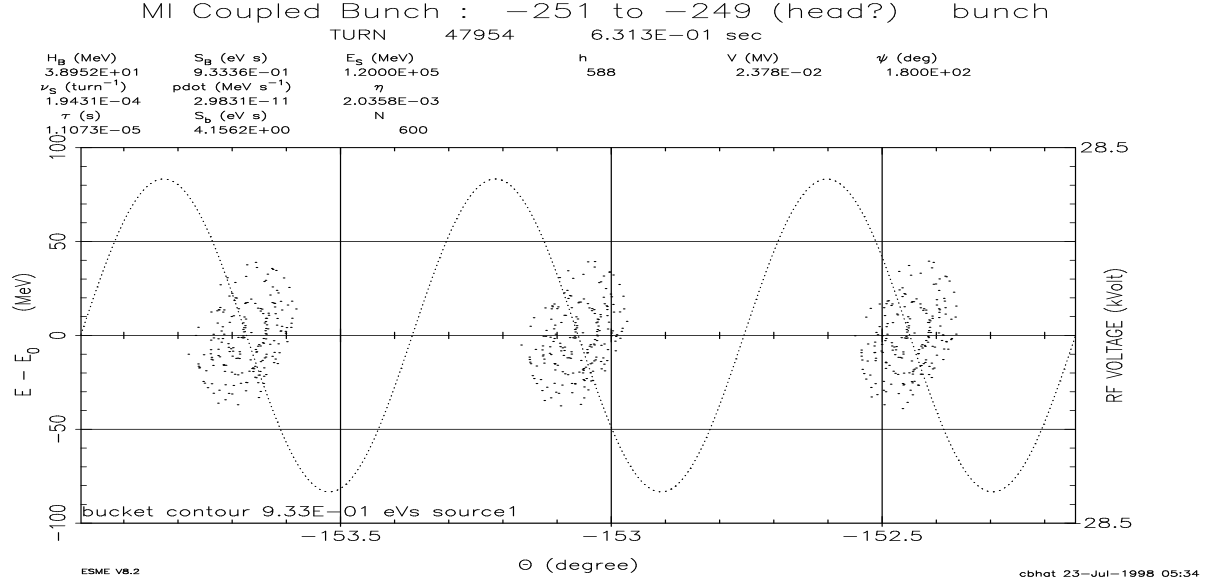


FIG. 6. Phase space distribution (top) first three and (bottom) last three bunches in a train of 504 bunches in the Main Injector after 0.539 seconds.



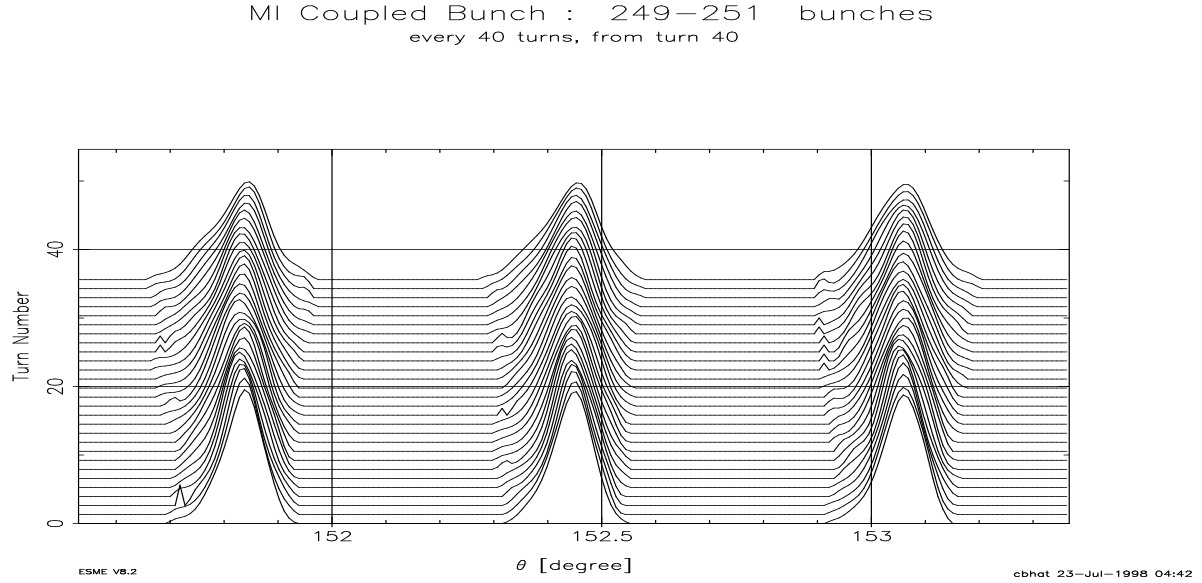
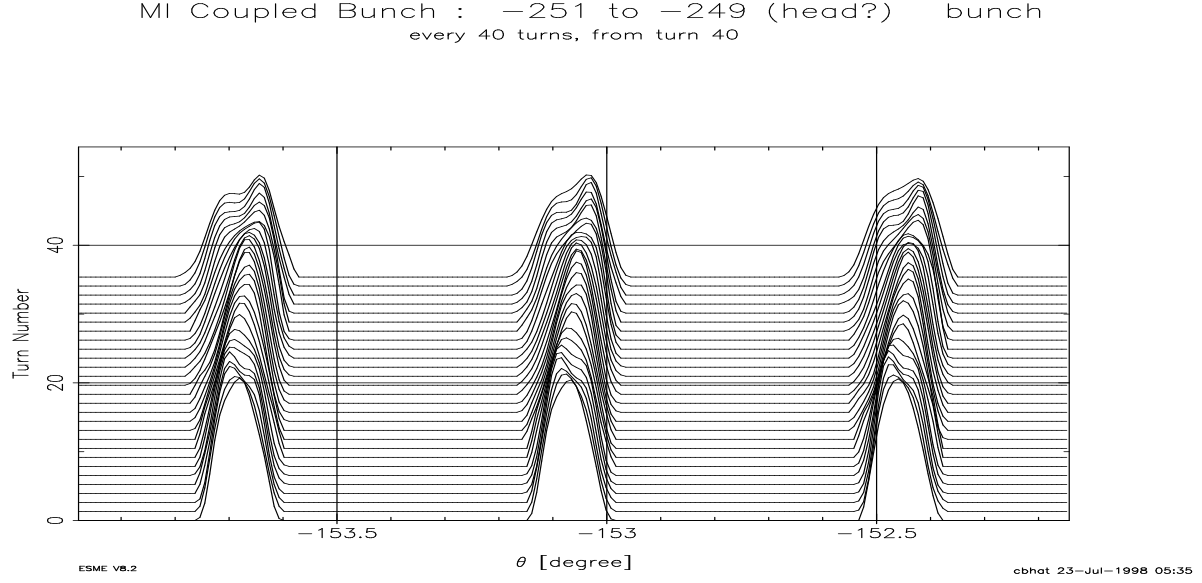


FIG. 7. Mountain range plots illustrating change in bunch length of (top) first three and (bottom) last three bunches in a train of 504 bunches in the Main Injector after 0.539 seconds (40 revolutions per trace).

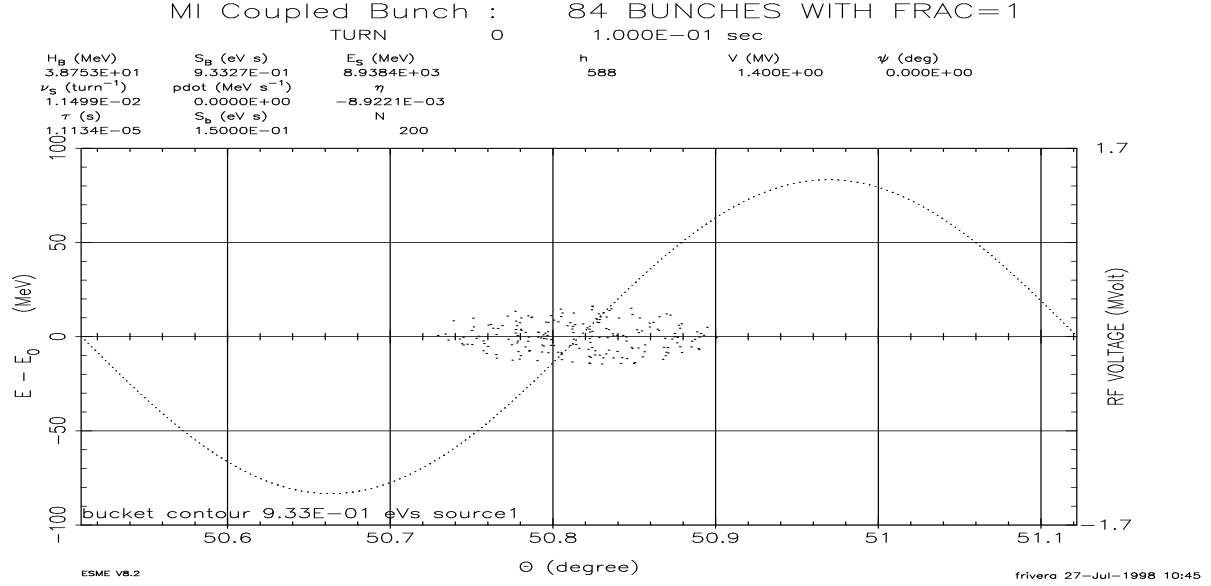
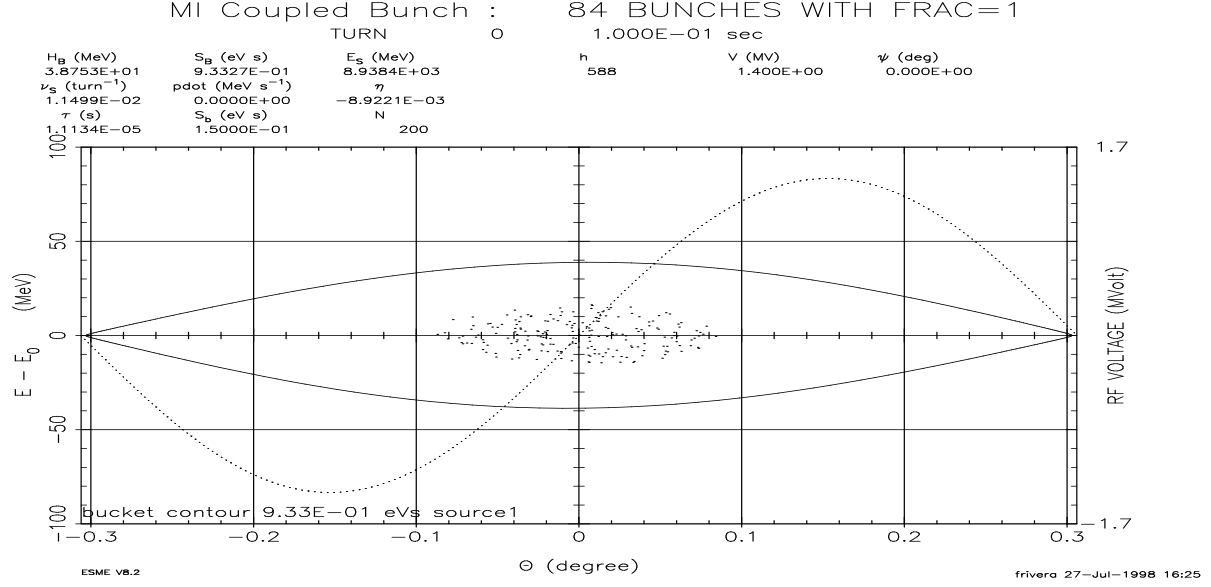
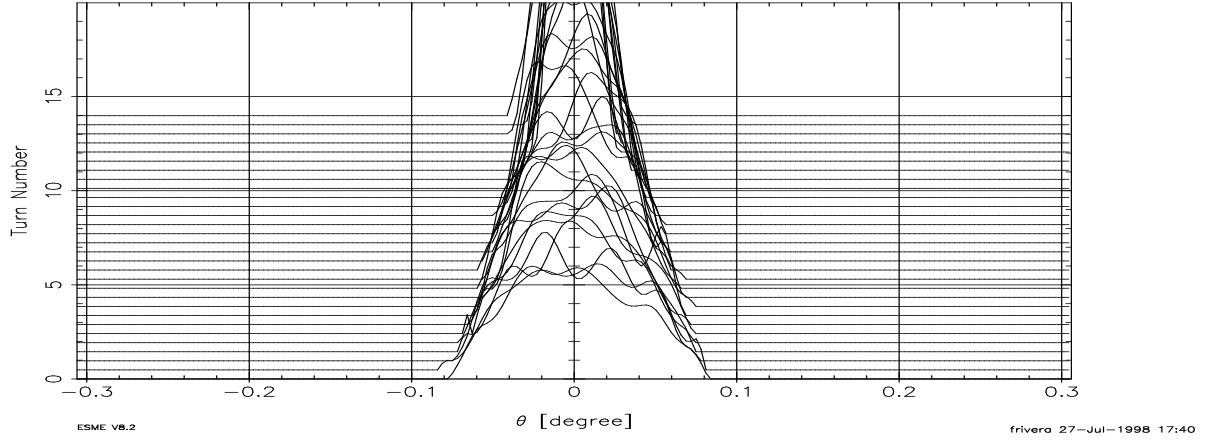


FIG. 8. Phase space distribution of (top) first and (bottom) last bunch in a train of 84 bunches in the Main Injector at injection time.

MI Coupled Bunch : 84 BUNCHES WITH FRAC=1  
every 324 turns, from turn 324



MI Coupled Bunch : 84 BUNCHES WITH FRAC=1  
every 324 turns, from turn 324

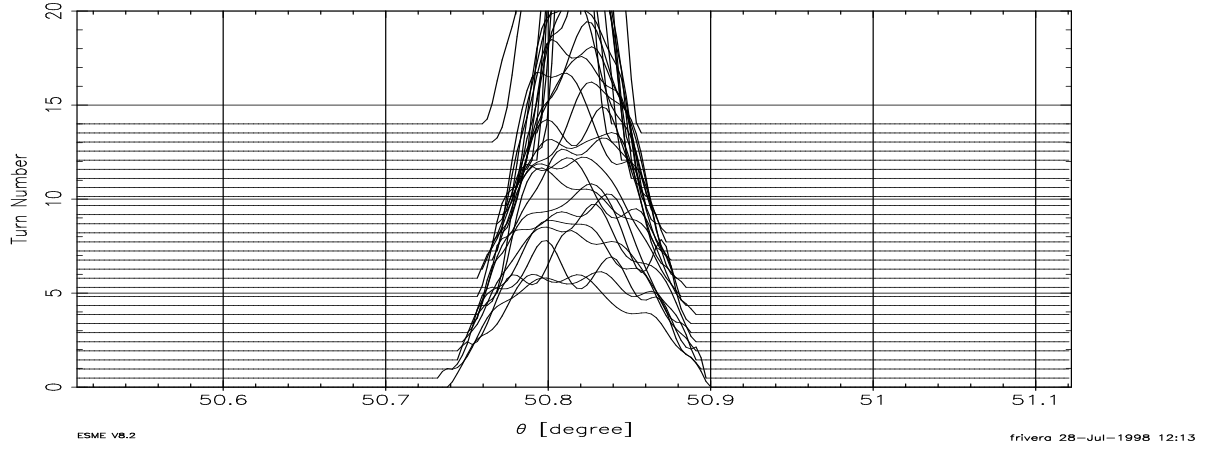


FIG. 9. Mountain range plots of (top) first and (bottom) last bunch in a train of 84 bunches in the Main Injector at injection time (324 revolutions per trace).

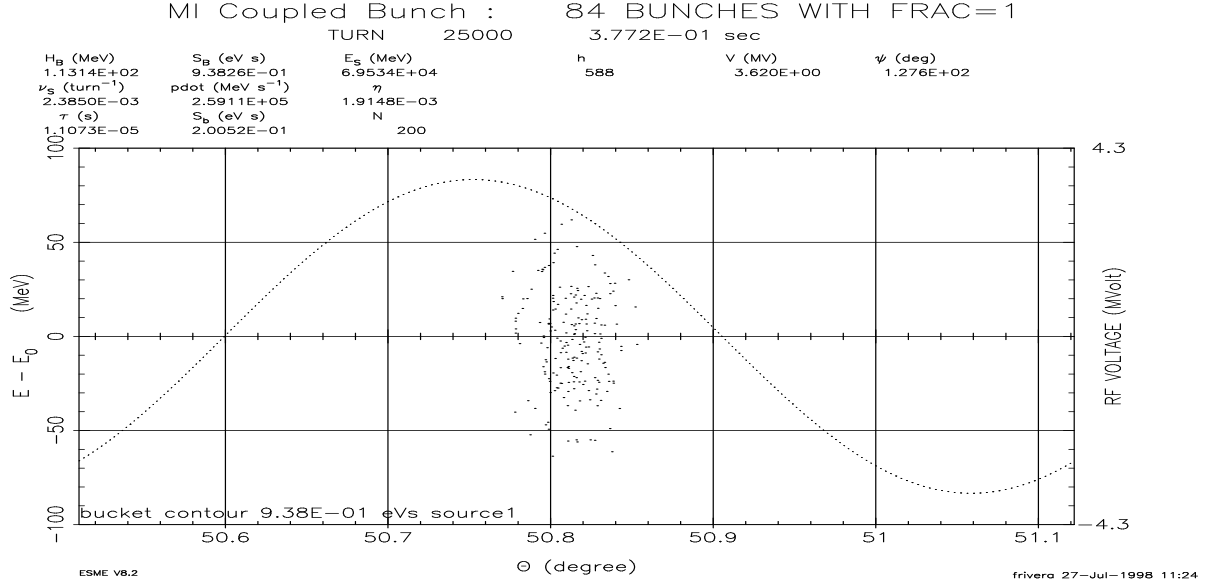
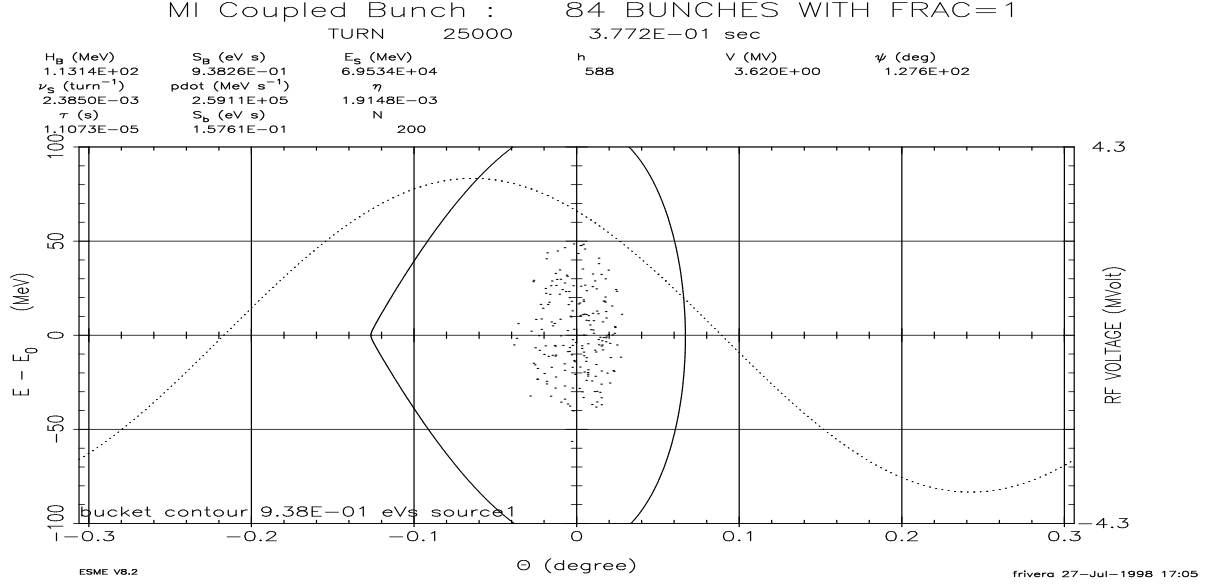


FIG. 10. Phase space distribution of (top) first and (bottom) last bunch in a train of 84 bunches in the Main Injector after 0.108 seconds of acceleration.

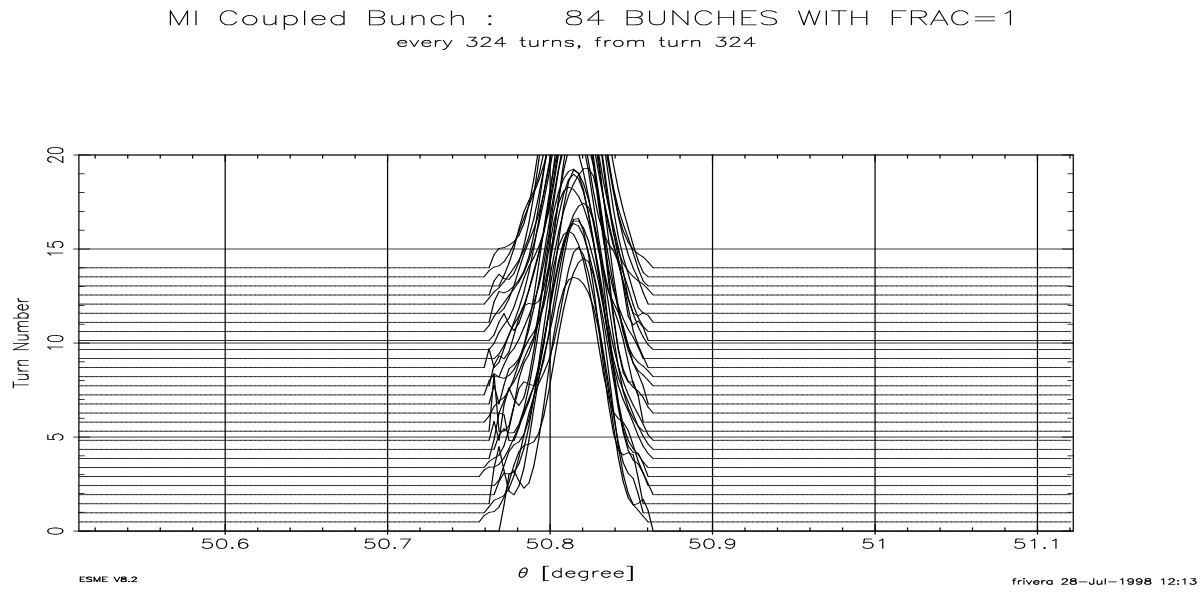
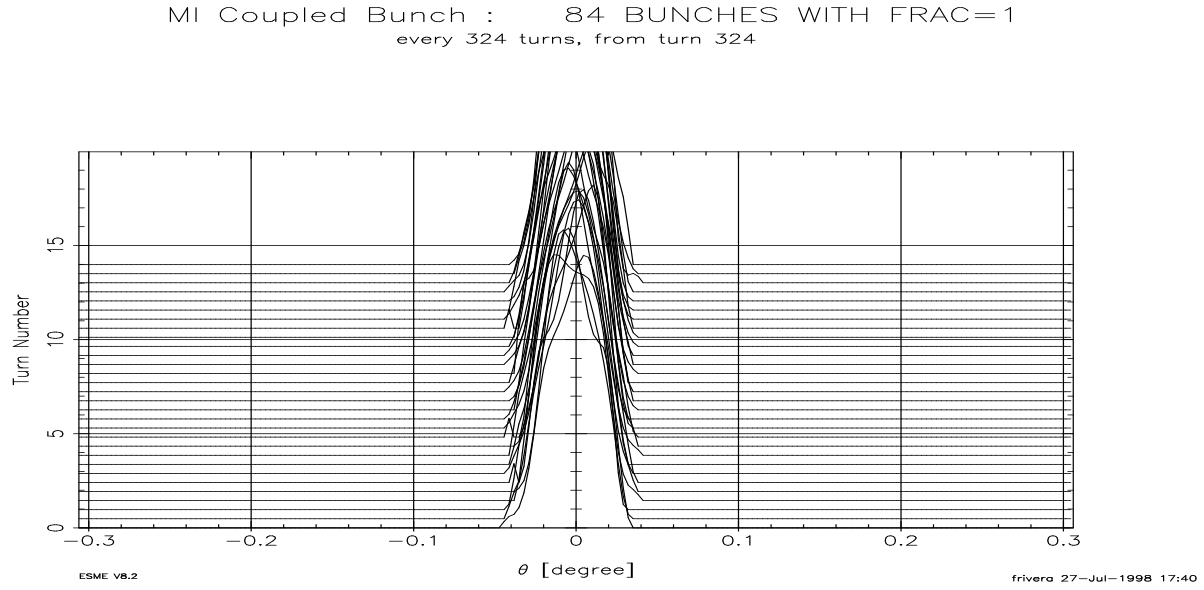


FIG. 11. Mountain range plots illustrating change in bunch length of (top) first and (bottom) last bunch in a train of 84 bunches in the Main Injector after 0.108 seconds of acceleration (324 revolutions per trace).

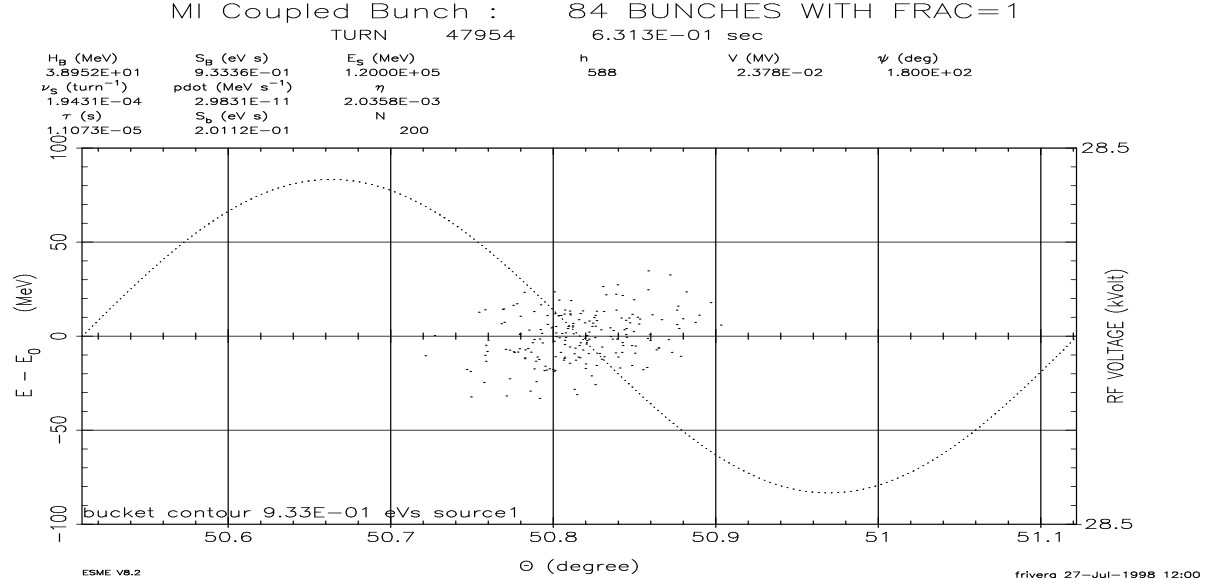
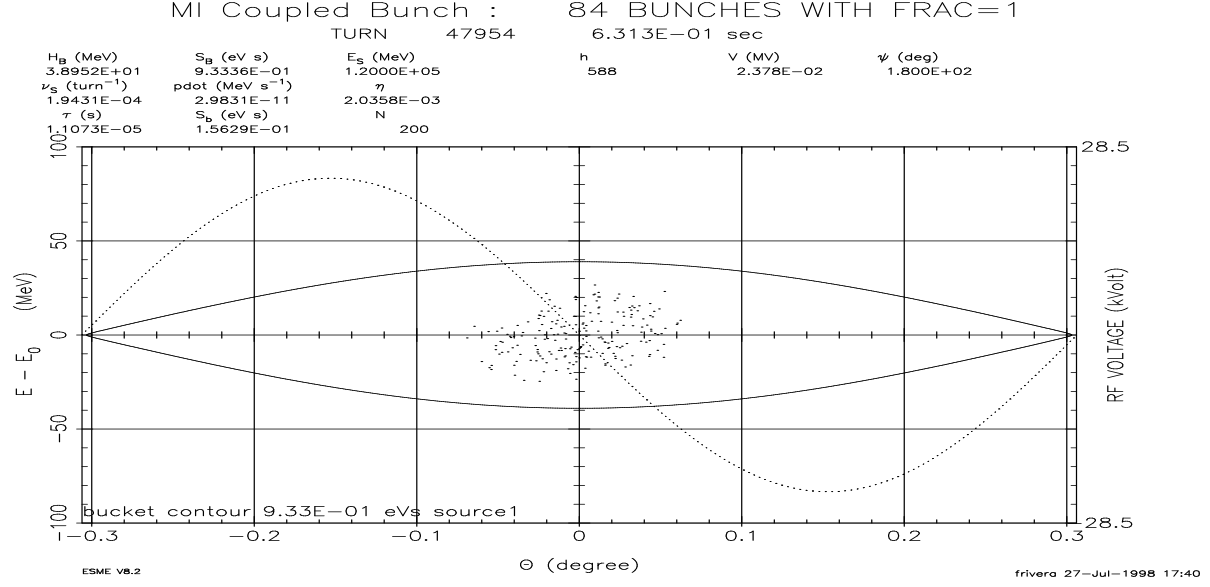


FIG. 12. Phase space distribution of (top) first and (bottom) last bunch in a train of 84 bunches in the Main Injector after 0.538 seconds.

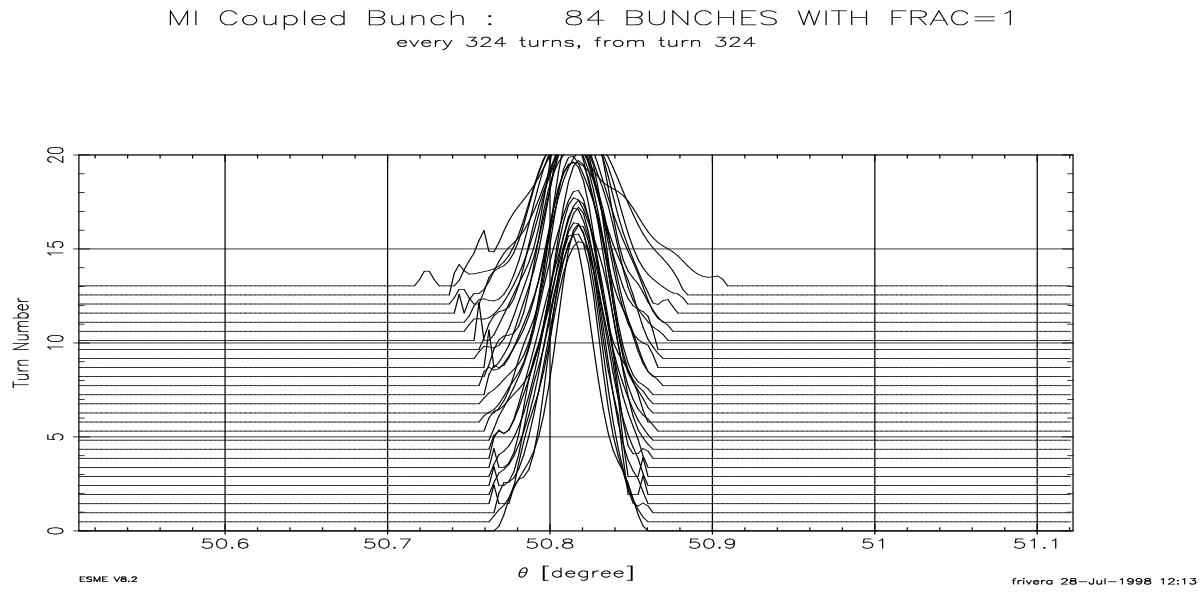
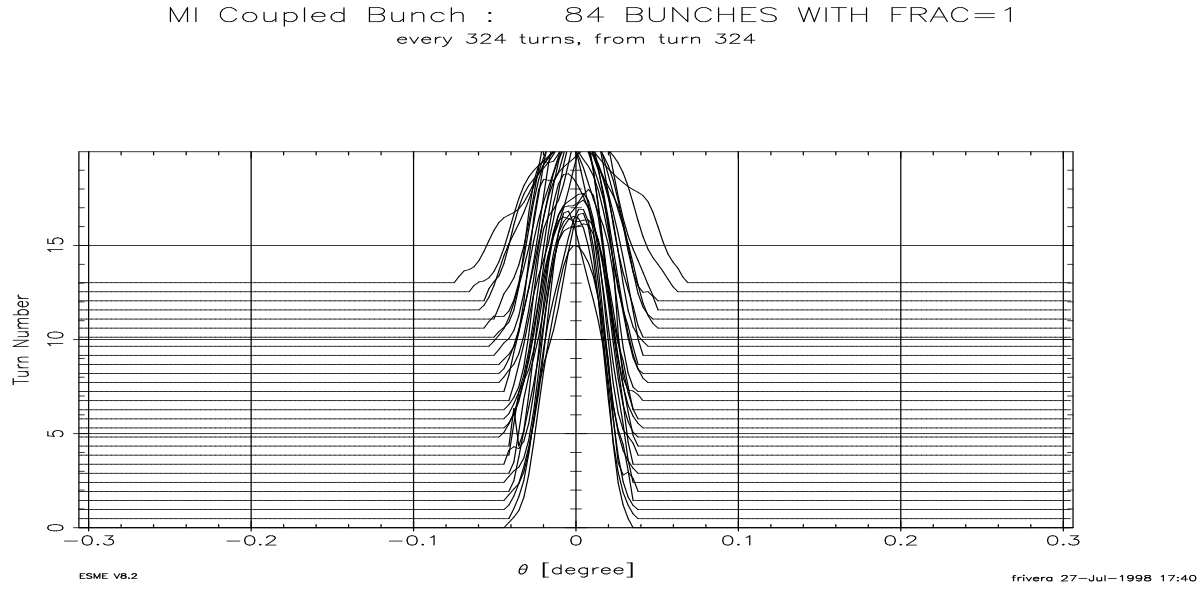


FIG. 13. Mountain range plots illustrating change in bunch length of (top) first and (bottom) last bunch in a train of 84 bunches in the Main Injector after 0.538 seconds (324 revolutions per trace).

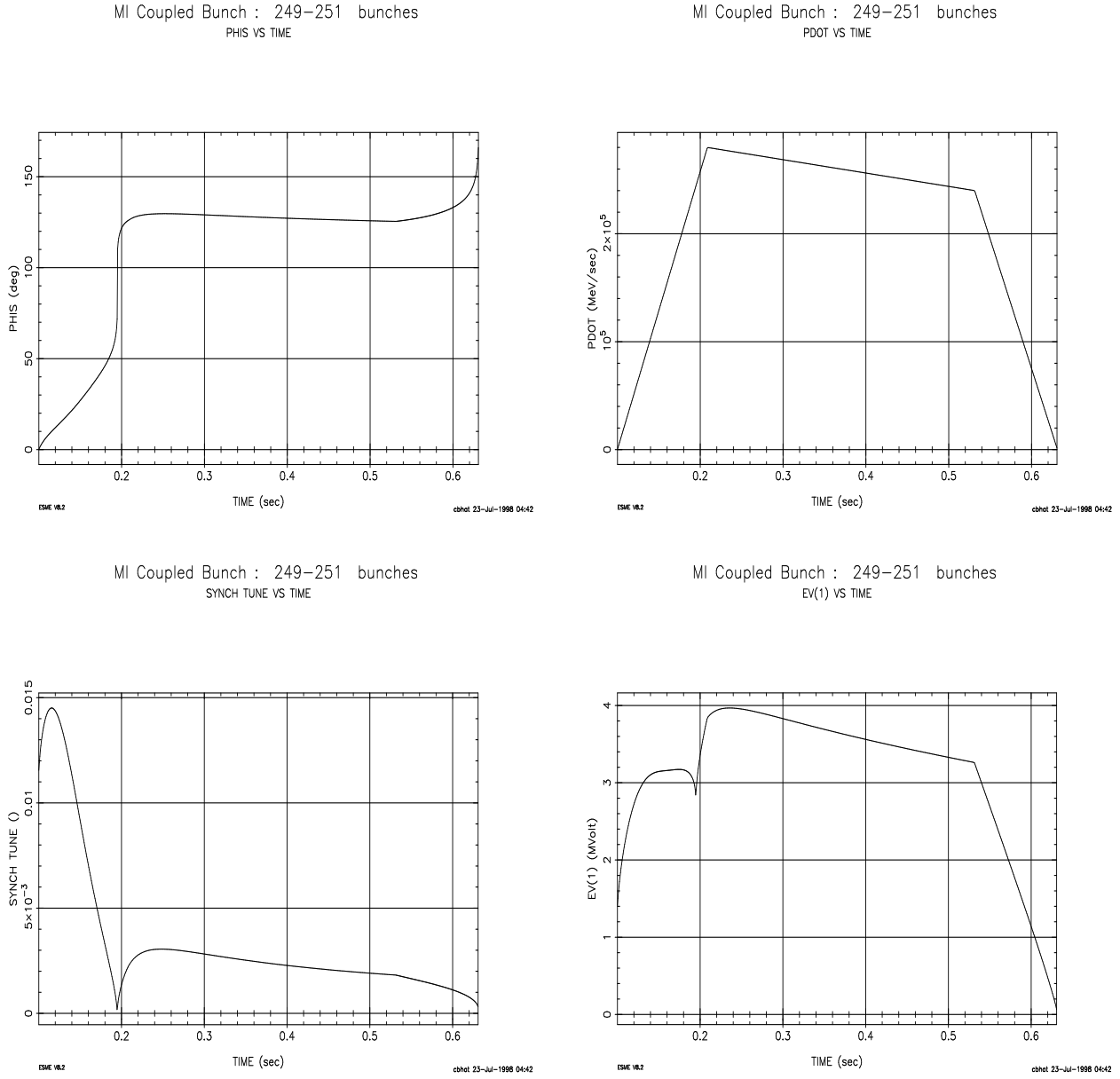


FIG. 14. Top left : Change in synchronous phase. Note that below transition (0.2sec) the angle is less than  $90^\circ$  and above transition it is more than  $90^\circ$ , Top right :  $dp_s/dt$ , the change in momentum versus time for the whole acceleration cycle, Bottom left : Synchrotron tune as a function of time. Here we can see how the synchrotron tune approaches zero close to transition (0.2sec), and Bottom right : RF voltage as a function of acceleration time.



### III. CONCLUSIONS

We have carried out simulations of longitudinal coupled bunch instability in the Main Injector including space charge effects and the first four prominent parasitic resonances in the MI rf cavities. Our preliminary analyses carried out using  $6 \times 10^{10}$  protons/bunch at longitudinal emittance of 0.15 eV-sec indicate that we should not encounter any considerable emittance growth or beam loss for  $\bar{p}$  production scenario. However, for 504 bunches we see considerable emittance dilution, particularly in the bunches in the tail region.

### IV. ACKNOWLEDGMENTS

I would like to thank my supervisor Chandra Bhat for his help on every step of the way. Thanks to Jim MacLachlan for many useful discussions and his help in setting up ESME to study coupled bunch instability. I also thank Dave Wildman and Joe Dey for providing necessary data on higher order resonances of MI rf cavity.

### V. REFERENCES

- [1] Fermilab Main Injector Technical Design Report (1994).
- [2] K Junck, J. Marriner et al., *A Study of the Coupled Bunch Instability in the Fermilab Main Ring*, Proceedings of the IEEE, 06/96, pp 3013-1015
- [3] S. Assadi, K. Junck et al., *Inference of Wakefield Structure by Driving Longitudinal Coupled Bunch Modes in Main Ring*, Proceedings of the IEEE, 06/96 pp 3016-3018
- [4] J Le Duff, *Longitudinal Beam Dynamics in Circular Accelerators*, CERN Accelerator School, Fifth General Accelerators Physics Course, S. Turner, CERN 94-01, Jan/1994, Vol 1, pp 289-311
- [5] W. T. Weng, *Fundamentals-Longitudinal Motion*, American Institute of Physics, 1989, pp 244
- [6] S. Ohnuma, *The Beam and the Bucket*, TM-1381, Jan/1986

- [7] “ A study of longitudinal instabilities and emittance growth in the Fermilab Booster synchrotron” by K. C. Harkey, (Ph. D. Thesis, Purdue University, 1993).
- [8] S. Stahl and S.A. Bogacz, *Coupled-bunch instability in a circular accelerator and possible cures: Longitudinal-phase-space simulation*, Phys. Rev. D **37**, 5 (03/1988), pp 1300-1036
- [9] J. Dey and D. Wildman, *Higher Order Modes of the Main Cavity at Fermilab*, Proceedings of the IEEE, 06/96, pp 1675-1677
- [10] J. A. MacLachlan, *Longitudinal Phase Space Tracking with Space Charge and Wall Coupling Impedance*, FN-446, Feb/1987
- [11] J. MacLachlan and J.-F. Ostiguy, *Enhancements to ESME*
- [12] J. MacLachlan, *Difference Equations for Longitudinal Motion in a Synchrotron*, FN-529, Dec/1989
- [13] J.M. Byrd, J. Corlett, *Spectral Characterization of longitudinal coupled-bunch instabilities at the Advanced Light Source*, Lawrence Berkeley Laboratory, May/1995
- [14] *Run II Design Handbook for FMI*, July/1995, V-32